Discovery of a Novel Class of Phosphodiesterase 10A Inhibitors and Identification of Clinical Candidate 2-[4-(1-Methyl-4-pyridin-4-yl-1*H*-pyrazol-3-yl)-phenoxymethyl]-quinoline (PF-2545920) for the Treatment of Schizophrenia[†]

Patrick R. Verhoest,* Douglas S. Chapin, Michael Corman, Kari Fonseca, John F. Harms, Xinjun Hou, Eric S. Marr, Frank S. Menniti, Frederick Nelson, Rebecca O'Connor, Jayvardhan Pandit, Caroline Proulx-LaFrance, Anne W. Schmidt, Christopher J. Schmidt, Judith A. Suiciak, and Spiros Liras

Neuroscience, Pfizer Global Research and Development, Eastern Point Road, Groton, Connecticut 06340

By utilizing structure-based drug design (SBDD) knowledge, a novel class of phosphodiesterase (PDE) 10A inhibitors was identified. The structure-based drug design efforts identified a unique "selectivity pocket" for PDE10A inhibitors, and interactions within this pocket allowed the design of highly selective and potent PDE10A inhibitors. Further optimization of brain penetration and drug-like properties led to the discovery of 2-[4-(1-methyl-4-pyridin-4-yl-1*H*-pyrazol-3-yl)-phenoxymethyl]-quinoline (PF-2545920). This PDE10A inhibitor is the first reported clinical entry for this mechanism in the treatment of schizophrenia.

Introduction

The phosphodiesterase (PDE[a]) gene family has led to the identification of drugable targets and treatments for various disease states. With the success of the PDE5 inhibitor sildenafil,[1] Pfizer initiated a gene family initiative to identify potential therapeutic utility for the 21 different human PDE genes.[2] Out of this effort, PDE10A was identified as a potential target for the treatment of central nervous system (CNS) disorders. PDE10A is highly expressed in the medium spiny neurons of the striatum[3] and has been shown to regulate both cGMP ($K_m = 7.2 \mu M$) and cAMP ($K_m = 0.26 \mu M$).[4] It is believed that inhibitors of PDE10A will regulate cyclic nucleotide signaling in the corticostriatothalamic circuit. It has previously been shown that PDE10A inhibitors are active in a variety of preclinical models that may predict efficacy in the treatment of schizophrenia.[5]

Although compounds with high PDE affinity have been readily identified, achieving high selectivity is still a key challenge. There are distinct differences in the full length structure of the PDEs, but it is not surprising that the catalytic domains that share a common function have a much more conserved structure. All the PDEs possess a common gluta-

mine, and for the dual substrate PDEs, this residue can rotate to form donor−acceptor hydrogen bonds to both cGMP and cAMP. There is a common hydrophobic clamp that is made up of lipophilic amino acids that form a stacking interaction with the purine-like heterocyclic core of both cGMP and cAMP. In addition, there is a common bimetal ion binding center that binds the phosphates of the cyclic nucleotides.[6]

PDE inhibitors have potential therapeutic utility but also have potential unwanted safety risks due to off-target PDE inhibition. Some examples that have been reported in the literature are with PDE6 inhibition and visual disturbances[7] and PDE3 inhibitors with cardiovascular changes.[8] A previous publication has highlighted the quinazoline series of PDE10A inhibitors, which were challenged with PDE3 selectivity issues.[9]

Results and Discussion

In an effort to identify a more selective class of PDE10A inhibitors, a diverse set of compounds from our internal compound collection were screened for PDE10A affinity. This effort identified triarylimidazole **1** (Figure 1), which has a PDE10A IC_{50} of 35 nM and displays >100× fold selectivity against the other PDEs.[10] Examination of its cocrystal structure with the PDE10A catalytic domain (Figure 2) revealed the basis for this extraordinary selectivity. It showed a binding interaction that is markedly different, not just from other PDE10A inhibitors but from PDE inhibitors in general. Unlike previously known PDE inhibitors, this inhibitor does not make a hydrogen bond with the conserved glutamine Gln-726.[2] Instead, the side chain amino nitrogen of Gln-726 is positioned directly above the center of one the methoxyphenyl groups, thus making a favorable amino−π interaction.[11] Most importantly for selectivity, the thiophene occupies a lipophilic pocket near the entrance of the hydrophobic cleft that defines the common PDE substrate binding site. Additionally, the imidazole accepts a hydrogen bond at

---

*To whom correspondence should be addressed. Phone: 860-686-2288. Fax: 860-686-0013. E-mail: patrick.r.verhoest@pfizer.com.

[a]Abbreviations: PDE, phosphodiesterase; SBDD, structure-based drug design; CNS, central nervous system; cGMP, cyclic guanosine monophosphate; cAMP, cyclic adenosine monophosphate; Tyr, tyrosine; Gln, glutamine; Leu, leucine; PDB, protein data bank; M_w, molecular weight; TPSA, topological polar surface area; HTS, high-throughput screen; LDA, lithium diisopropyl amine; THF, tetrahydrofuran; CYP, cytochrome P450; PgP, P-glycoprotein; SC, subcutaneous; LE, ligand efficiency; LLE, lipophilic ligand efficiency; CAR, conditioned avoidance response; MED, minimal effective dose; ADME, absorption distribution metabolism and excretion; HBE, hydrogen bond energy.

the top of the pocket from the OH of Tyr-693, which accepts a hydrogen bond from the carbonyl of conserved Gln-726.

A comparison of the known PDE crystal structures and profiling the inhibitor binding site led us to determine that the
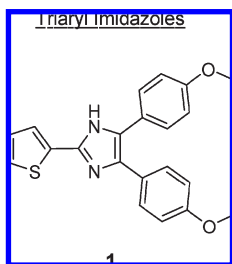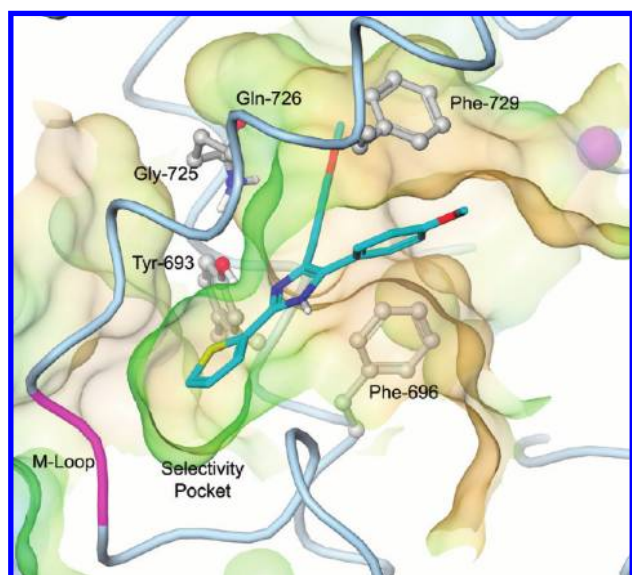

Figure 1. Structure of triaryl imidazole **1**.

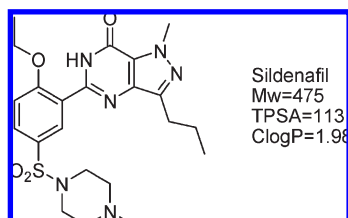**Figure 2.** Compound **1** (PDB 3HQW) bound in PDE10A selectivity pocket.

Figure 3. Structure of sildenafil.

lipophilic pocket occupied by the thiophene group is unique to PDE10A in the PDE family for the following reasons. First, among all the 21 PDE family proteins, only PDE10A has a glycine residue at position 725, next to the conserved gluta-mine.[2] The presence of a larger side chain in all other PDEs blocks access to this lipophilic pocket. In addition, the resi-dues that form the back of this lipophilic pocket are from the M-loop, which connects helix 14 and 15. Because of an insertion, this loop is longer in PDE10A than all the other PDEs except PDE5 and PDE6, which results in this pocket being deeper in PDE10A than all other PDEs. Finally, PDE10A has Tyr-693 to form a hydrogen bond interaction with which to anchor an inhibitor in this pocket. In addition to PDE10A, this potential hydrogen bonding group is only found in PDE2, where access to this pocket is blocked by a leucine residue of PDE2.

Utilizing the structural knowledge of how to obtain selec-tivity for PDE10A, we implemented a strategy to develop multiple chemical series to address attrition risks. We had been focusing on multiple chemical series, but none of these bound in the selectivity pocket and possessed the desired physiochemical properties.[12] After the biological confidence in rationale was built through the quinazoline and triaryl imidazole series, we undertook a full file high-throughput screen (HTS). To identify lead series with built in selectivity, we only pursued diverse hits from this screen that had potential to bind in the PDE10A selectivity pocket and to form a hydrogen bond with Tyr-693. To confirm our hypoth-esis, we subjected promising hits to X-ray crystallography to unambiguously identify their binding modes. In addition, we focused on identifying lead structures with drug-like physio-chemical properties. We targeted leads that had a molecular weight less than 400, were only moderately lipophilic with a ClogP ≤ 4, and contained a minimum number of hydrogen bond donors to increase our probability of achieving brain penetration. These physicochemical targets are a major change from the PDE5 inhibitors that are on the market.[13] Compounds like sildenafil (Figure 3) have difficulty accessing the CNS compartment due to their size ($M_w = 475$) and polarity (TPSA = 113).

Out of this high-throughput screen, we found multiple chemical series that met our desired criteria. One that was rapidly prosecuted is exemplified by novel pyrazole com-pound **2** (Figure 4). In this case, the X-ray crystal structure of **2** confirmed the quinoline formed a hydrogen bond to the desired tyrosine and occupied the "selectivity" pocket (Figure 5). Pyrazole **2** was a fairly efficient inhibitor (ligand efficiency = 0.37)[14] of PDE10A with an IC_{50} of 11.5 nM and possessed reasonable physicochemical properties with a mo-lecular weight of 392 and a ClogP of 4. Further screening guided by SBDD led us to identify compound **3**, where the
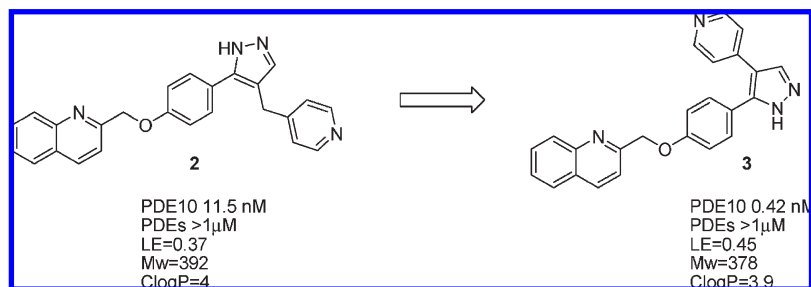

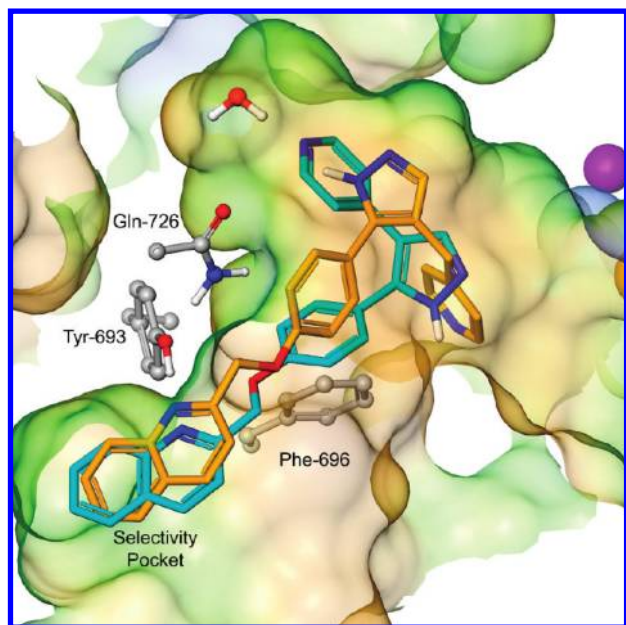**Figure 4.** Identification of HTS hit **2** and lead pyrazole **3**.

Figure 5. Cocrystal structure of **2** (yellow, PDB code 3HQY) bound to the PDE10A catalytic site. Cocrystal structure of **3** (blue, PDB code 3HQZ) is overlaid.
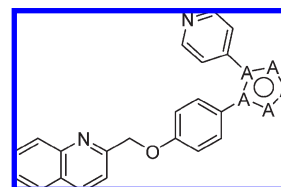
Table 1. PDE10A Potency for Core Heterocycles

#	A	PDE10A[a]	#	A	PDE10A[a]
3		0.42	**12**		4.76
9		0.37	**13**		1.41
10		1.54	**14**		11.7
11		0.92	**15**		1690

[a] PDE10A IC_{50} Potency reported in nM.

methylene has been excised. Pyrazole **3** is a subnanomolar PDE10A inhibitor with an IC_{50} of 0.42 nM and exhibits $> 1000\times$ selectivity over the other PDEs.

This series of pyrazoles represents a nonclassical binding mode for a PDE inhibitor. They do not form a hydrogen bond interaction with the conserved glutamine as most PDE5 and PDE4 inhibitors do. Pyrazole **3** maintains the hydrogen bond to the tyrosine and occupies the PDE10A selectivity pocket but goes deeper into a pocket behind the conserved glutamine than HTS hit **2**. The pyridyl nitrogen also forms a hydrogen bond to a water molecule (2.6 Å) that is hydrogen bound to the PDE10A backbone. This deeper penetration of an additional binding pocket and the hydrogen bond to the water molecule may help explain the significant increase in potency that is seen with compound **3**.

Synthesis of **3** was completed starting with 4-hydroxyl benzoic acid methyl ester **4** and alkylating with 2-chloromethyl quinoline followed by hydrolysis to afford the desired acid **5**. Activation of the acid with thionyl chloride and Weinreb amide formation provides the coupling partner **6** in good yield.[15] The anion of 4-picoline (2 equiv) was formed with lithium diisopropyl amide (LDA) and added to a tetrahydrofuran (THF) solution of the Weinreb amide coupling partner. Two equivalents of the anion were necessary to achieve an acceptable yield of **7** (80%). Following treatment with dimethoxymethyl-dimethyl amine to form the enaminone **8**, hydrazine was added to form the desired pyrazole compound **3**.

Compound **3** is an excellent lead structure with improved potency over compound **2**. It also shows a reduced drug−drug interaction liability with less CYP3A4 inhibition ($IC_{50} > 10 \mu$M vs 450 nM compound **2**) due to the sterics around the pyridyl nitrogen and the deactivation of the pyridine by conjugation to the pyrazole.[16] While this lead compound had the requisite potency and selectivity, it fell short of a drug candidate in terms of its in vivo efficacy. It raised cGMP levels in the striatum 350% at 10 mg/kg and was active in the conditioned avoidance response task (CAR)[17] with an ED_{50}

of 5 mg/kg (SC) but required a high free plasma concentration in mice (15 nM) in relation to the PDE10A potency (0.42 nM) to achieve activity. The high ratio of free plasma exposure relative to the enzyme IC_{50} (36×) to produce the desired biochemical and behavioral effect was the result of modest brain penetration (brain/plasma = 0.21). These higher free and total drug levels could lead to an increase in safety risks and led to a higher dose projection to sustain efficacy in humans. These liabilities directed us to identify compounds with improved CNS penetration.

Our strategy to improve brain penetration was to maintain molecular weight and remove the hydrogen bond donor present in pyrazole **3**. The enaminone **8** (Scheme 2) afforded a versatile intermediate to rapidly synthesize compounds with this desired profile. Treatment with small hydrazines afforded substituted pyrazoles and addition of hydroxyl amine provided an isoxazole. In addition, treatment with amidines delivered pyrimidines, which allowed us to determine the optimal ring size of the core heterocycle.

The SAR for the pyrazole and pyrazole replacements that remove the hydrogen bond donor was very promising (Table 1). Substitution of the pyrazole with simple alkyl groups retained potency while adding minimal molecular weight. The simple methyl substituted pyrazole **9** (PF-2545920)[18] proved to be 0.37 nM and in an in vitro P-glycoprotein (PgP) overexpressing cell line had improved the efflux ratio from 2.3 to 1.0.[19] We expected that this reduced PgP liability would improve our brain penetration and in vivo efficacy. The pyrazole heterocycle was the most potent of the five-membered heterocycles prepared, with isoxazole **14** displaying a significant loss in potency. The pyrimidine analogues were also significantly less active than **3**, potentially due to the decreased bond angle between the phenyl and pyridine rings. This may prohibit the pyridine ring from making a key hydrogen bond to a tightly bound water molecule.

To test the hypothesis that the pyridyl hydrogen bond to the water molecule was crucial for PDE10A affinity,

Table 2. PDE10A Potency of Aryl Pyridyl Replacements and Calculated Hydrogen Bond Energy
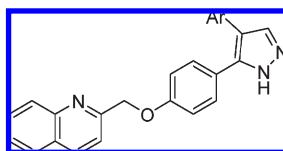
#	Ar	PDE10A[a]	ΔG[b] (kcal/mol)	Hydrogen Bond Energy (kcal/mol)	#	Ar	PDE10A[a]
3		0.42	-12.75	-6.68	18		258
16		27.2	-10.29	-5.88	19		371
17		11.9	-10.78	-6.08	20		413

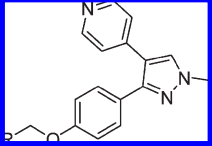[a] PDE10A IC$_{50}$ potency in nM. [b] $\Delta G = RT \ln(K_d) \approx 1.36 \log(IC_{50})$, at $T = 298$ K.
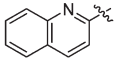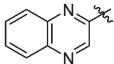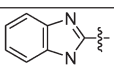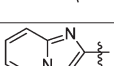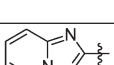
Scheme 1. Synthesis of Lead **3**[a]
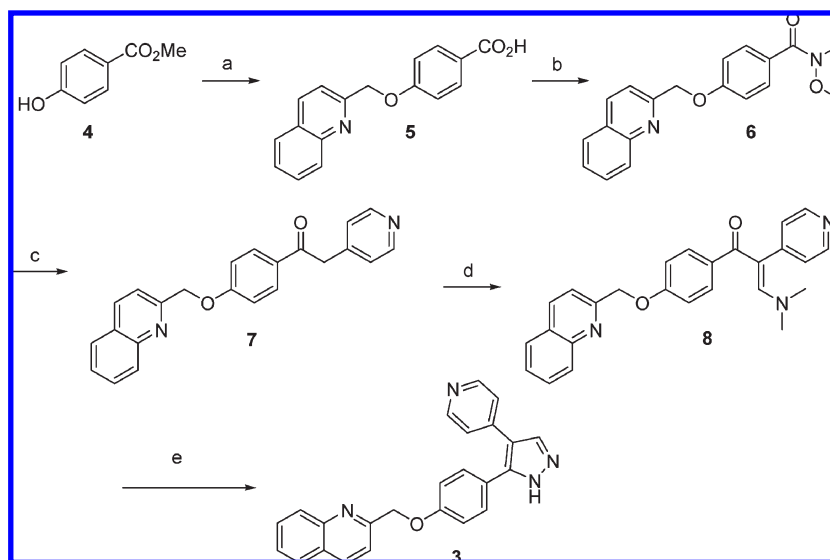
[a] Reagents and conditions: (a) 2-chloromethyl quinoline, K_2CO_3, acetone, reflux, 16 h, then MeOH, 1 N NaOH 16 h (60% 2 steps); (b) thionyl chloride 3 h, then THF, triethylamine, NHMeOMe, 18 h (87%), (c) 4-picoline, LDA, −78 to rt (80%); (d) dimethoxymethyl-dimethyl amine, reflux, 1 h; (e) MeOH, hydrazine, reflux 1 h (82%, 2 steps).

aromatic and heteroaromatic replacements for the pyridine ring were designed. Compounds **16**−**20** (Table 2) were synthesized from the Weinreb intermediate **6** (Scheme 1) utilizing the anion chemistry that has previously been described. As predicted by the X-ray crystal structure, compounds **18** and **19** that could not accept a hydrogen bond to the water were significantly less active. The two heterocyclic analogues that could form a hydrogen bond, pyrimidine **16** and pyridazine **17**, retained good affinity but were significantly less potent than **3**.

To further understand the SAR discrepancy of **16** and **17**, the nitrogen hydrogen bond strengths of the heterocycles were computationally estimated. Ligand binding is a complex process, and binding energy contains contributions from multiple components such as ligand and protein interactions, conformational strain, and desolvation. For a closely related congeneric series of compounds, we assumed similar contributions from one or more of these binding components. In particular, if we assume most of the energetic terms are similar for compounds **3**, **16**, and **17** except for the ability of each heterocycle to make a hydrogen bond to the water molecule in the active site, we could computationally test this hypothesis by calculating their hydrogen bond strength. The hydrogen bond energy was computed by applying pseudospectral local second-order Moller−Plesset or the PS-LMP2 method.[20] The model system was built by using the crystal water bound to the pyridyl nitrogen and the corresponding heterocycle derivatives. The structures were optimized with X3LYP/6-31G**,

Table 3. PDE10A Potency of Quinoline Replacements

#	R	PDE10A[a]	Clint (uL/min/mg)	ClogP	LLE
9	(quinolin-2-yl)	0.37	37.2	3.84	5.59
25	(quinoxalin-2-yl)	5.09	16	3.09	5.20
26	(1-methylbenzimidazol-2-yl)	1.29	85	3.39	5.49
27	(imidazo[1,2-a]pyridin-2-yl)	0.79	38	3.22	5.88
28	(triazolo-pyridin-2-yl)	3.40	<7	2.32	6.14

[a] PDE10A IC$_{50}$ potency in nM.

Scheme 2. Heterocycle Synthesis

Figure 6. Subcutaneous dose response of **9** in the condition avoidance response assay (statistical analysis comparing drug to vehicle: $p = 0.012$ at 1.78 mg/kg, $p = < 0.01$ at 3.2 mg/kg).

Scheme 3. Synthesis of Quinoline Replacement Analogues

Reagents and conditions: (a) thionyl chloride 3 h, then THF, triethylamine, NHMeOMe, 18 h (99%), 4-picoline, LDA, −78 to rt (73%); (b) dimethoxymethyl-dimethyl amine, reflux, 1 h, then MeOH, methyl hydrazine, reflux 1 h (45%, 2-steps, major isomer); (c) H$_2$, Pd(OH)$_2$, ethanol/EtOAc (91%); (d) AR−OH, ditertbutyldiazocarboxylate, PPh$_3$ (67−96%).
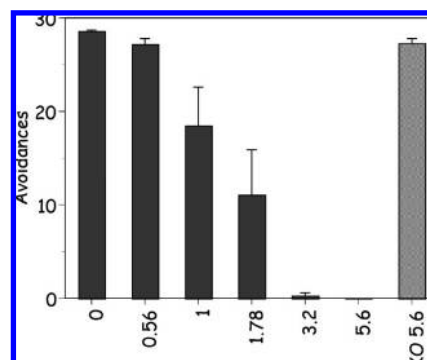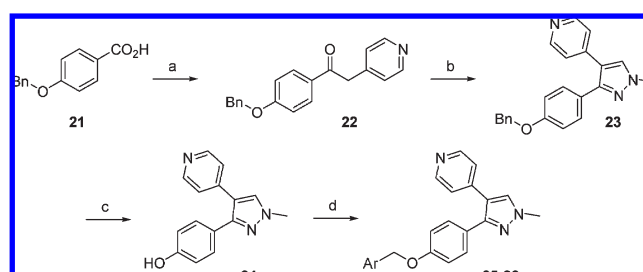
and the binding energies were calculated using two correlation-consistent basis sets (cc-pVTZ(-f) and cc-pVQZ(-g)) and LMP2 theory, including corrections for the basis set superposition error.[21] As expected, pyridyl **3** calculates to have a stronger interaction with the crystal water (Table 2) by more than 0.5 kcal/mol of energy. It is interesting to note that this calculation correctly predicts the rank order of the compounds in terms of potency but does not predict the absolute potency difference seen between **3** and **16**/**17**.

In an effort to understand how lipophilicity affected human liver microsomal intrinsic clearance in this series, compounds **25**−**28** (Table 3) were designed that replaced the quinoline ring with a more polar bicyclic aromatic group.[19] To rapidly prepare these desired targets compound **24** was synthesized (Scheme 3) utilizing similar chemistry that has been described in Scheme 2. From the phenol, coupling with the heteroaromatic benzyl alcohols utilizing Mitsonobu chemistry afforded compounds **25**−**28**.

Out of this effort, potent compounds with both 9- and 10-membered bicyclic aromatic groups with lower ClogP were identified. As intended, some of these analogues showed reduced human liver microsomal intrinsic clearance compared to the parent. Compound **28** was not metabolized by human liver microsomes, and compound **25** displayed significantly less

metabolic liability. In addition, these compounds maintained or improved their lipophilic ligand efficiency (LLE), which is a measure of potency for lipophilicity (LLE = −logK_i − ClogP) (Table 3).[22] Although there was an improvement in intrinsic clearance and LLE, none of the compounds provided a significant improvement over compound **9**.

Our extensive SAR efforts confirmed that **9** possessed the most attractive attributes. Thus, compound **9** was put through a battery of in vivo behavioral models and shown to be efficacious. As designed by removing the hydrogen bond donor in compound **3** and replacing it with a methyl, **9** demonstrated improvements in CNS penetration. The brain to plasma ratio in a mouse increased from 0.21 to 0.86. In the conditioned avoidance response assay (CAR), **9** was active with an ED$_{50}$ of 1 mg/kg (Figure 6) at a significantly lower total plasma exposure (115 nM) than compound **3**. It is highly protein bound, showing efficacy at a free plasma exposure of 0.3 nM. It was also inactive in the PDE10A knockout mice, providing evidence that the efficacy is mediated through PDE10A inhibition.

The effects on cyclic nucleotide signaling in the striatum were measured with subcutaneous dosing of **9** in mice. The striatum section of the brain was chosen as the tissue due to the high expression levels of PDE10A. Administration of **9** to mice caused a dose dependent increase in striatal cGMP (Figure 7). The minimal effective dose (MED) was ∼1 mg/kg, which elevated cGMP ∼3 fold. The elevation in cGMP appears to plateau and displays a maximal elevation of approximately a 5-fold increase at 3.2 mg/kg.
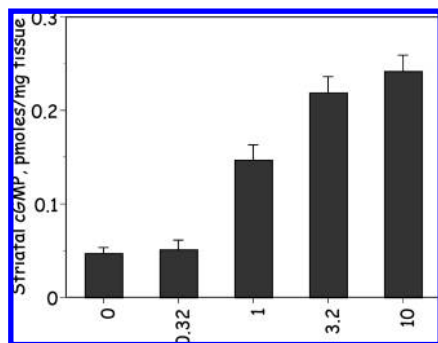
Figure 7. Subcutaneous dose response of **9** in the striatal cGMP assay.

Species	Dose (mg/Kg)	Route	CLh (ml/min/Kg)	Vdss (L/Kg)	T1/2 (h)	%F
Rat Sprague-Dawley	0.1	IV	36	2.3	2.1	
	1.0	PO			1.4	30
Dog Beagle	0.3	IV	7.2	1.7	6.3	
	0.1	PO			7.1	100
	3.0	PO			4.3	68
Monkey Cynomolgus	0.03	IV	13.9	0.56	0.6	

Figure 8. In vivo pharmacokinetic properties of **9**.
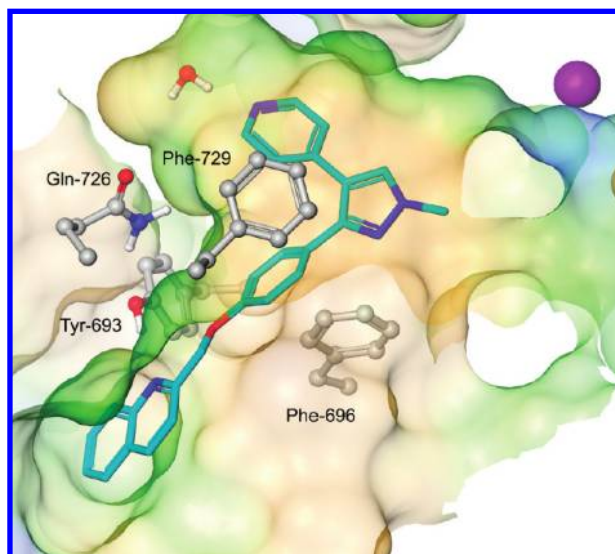

Figure 9. Compound **9** bound in PDE10A pocket (PDB 3HR1).

With **9** displaying efficacy in vivo, a high degree of PDE selectivity ($>1000\times$) and selectivity in the CEREP panel ($>100\times$), we explored its pharmacokinetic properties in multiple preclinical species (Figure 8). Overall, it displays low to moderate in vivo clearance with a moderate volume of distribution. Absorption of **9** following oral administration of a single dose was variable in preclinical species, with an absolute bioavailability of 30% in rats to 68−100% in dogs. This encouraging preclinical data together with the human in vitro ADME properties suggested that **9** would possess desirable drug-like human pharmacokinetic properties.

Conclusion

On the basis of the exciting preclinical data, **9** has entered clinical trials for the treatment of schizophrenia.[23] It is the first reported clinical entry for this exciting new mechanism.

In summary, structure-based drug design efforts utilized a novel binding pocket to identify a selective class of PDE10A inhibitors (Figure 9). This class possessed distinct physicochemical properties from the marketed PDE5 inhibitors, and this series was optimized for potency, selectivity, in vivo efficacy, CNS penetration, and pharmacokinetics to yield **9**. It is a highly potent and selective PDE10A inhibitor with excellent in vivo efficacy in neurochemical elevation of cyclic nucleotides and in models predictive of antipsychotic activity. The preclinical pharmacokinetic properties were very promising. With the entry of **9** into clinical trials, we plan to determine if PDE10A inhibition can improve schizophrenic patient outcomes.

Experimental Section

All reagents and solvents were used as purchased from commercial sources. Reactions were carried out under a blanket of nitrogen. Silica gel chromatography was done using the appropriate size Biotage prepacked silica filled cartridges. Mass spectral data was collected on a Micromass ADM atmospheric pressure chemical ionization instrument (LRMS APCI). NMR spectra were generated on a Varian 400 MHz instrument. Chemical shifts were recorded in ppm relative to tetramethylsilane (TMS) with multiplicities given as s (singlet), bs (broad singlet), d (doublet), t (triplet), dt (double of triplets), and m (multiplet). Compound purity is determined by combustion analysis (Quantitative Technologies inc.) or high pressure liquid chromatography (HPLC). HPLC conditions utilized are as follows. Gradient: 0−0.25 min 5%A:95%B, 0.25−6.25 min 5%A:95%B => 90%A:10%B, 6.25−6.75 min 90%A:10%B, 6.75−6.85 min 90%A:10%B => 5%A:95%B, 6.85−9.5 min 95%A:5%B; column temp: 45 °C. UV detector: 210 nM. Retention times (RT) are in minutes and purity is calculated as % total area. (Column 1: Waters BEH C8 2.1 mm × 100 mm 1.7 um; mobile phase A: acetonitrile, B: 0.1% (v/v) H_3PO_4 + 50 mM $NaClO_4$. Column 2: Waters BEH C8 2.1 mm × 100 mm 1.7 um; mobile phase A; acetonitrile, B: 20 mM ammonium bicarbonate pH 6.8. Column 3: Waters BEH RP C18 2.1 mm × 100 mm 1.7 um; mobile phase A: acetonitrile, B: 0.1% methanesulfonic acid. Column 4: Waters HSS T3 2.1 μm × 100 1.8 μm; mobile phase A: acetonitrile, B: 0.1% methanesulfonic acid. Column 5: Waters BEH C8 2.1 mm × 100 mm 1.7 μm; mobile phase A; acetonitrile, B: 20 mM ammonium bicarbonate pH 8.0. All final compounds either met combustion analysis within ±0.4% or were >95% purity by HPLC.

4-(Quinolin-2-ylmethoxy)-benzoic Acid Methyl Ester. To a solution of 2-chloromethyl quinoline (2 g, 9.3 mmol) in acetone (47 mL, 0.2M) was added 4-hydroxy benzoic acid methyl ester **4** (1.42 g, 1.0 equiv) and potassium carbonate (3.86 g, 3 equiv). The reaction mixture was heated at 60 °C for 16 h under N_2 atmosphere, cooled to ambient temperature, and poured into 1 N sodium hydroxide (50 mL)/ethyl acetate (100 mL). The layers were separated and the organic layer dried with magnesium sulfate, filtered, and concentrated. Biotage MPLC was run using a 5−30% ethyl acetate/hexane gradient on a 40 M column to provide the title compound as a white solid (1.66 g, 61%). ^{1}H NMR (400 MHz, CDCl$_3$) δ 8.18 (d, $J = 8.7$ Hz, 1 H), 8.07 (d, $J = 8.3$ Hz, 1 H), 7.95 (m, 2H), 7.82 (d, $J = 7.9$ Hz, 1 H), 7.74 (dt, $J = 7.1, 1.7$ Hz, 1 H), 7.62 (d, $J = 8.3$ Hz, 1 H), 7.55 (dt, $J = 7.9, 1.2$ Hz, 1 H), 7.03 (d, $J = 9.1, 2$ H), 5.41 (s, 2 H), 3.84 (s, 3 H); MS: (M^+H $m/z = 294.2$).

4-(Quinolin-2-ylmethoxy)-benzoic Acid (5). To a solution of 4-(quinolin-2-ylmethoxy)-benzoic acid methyl ester (500 mg, 1.7 mmol) in tetrahydrofuran (8.5 mL) and methanol (3 mL) was added 1 N NaOH (3.4 mL, 2 equiv). The reaction mixture was stirred at ambient temperature for 16 h. To the reaction mixture was added 50 mL of brine and the pH was adjusted to 3 with 1 N HCl to provide a white precipitate, which was filtered and dried to provide the title compound as a white solid

(463 mg, 98%). ^{1}H NMR (400 MHz, DMSO) δ 8.39 (d, J = 8.3 Hz, 1 H), 7.99 (m, 2 H), 7.81 (m, 2H), 7.76 (dt, J = 8.3, 1.7 Hz, 1 H), 7.64 (d, J = 8.3 Hz, 1 H), 7.60 (dt, J = 7.9, 1.3 Hz, 1 H), 7.12 (M, 2 H), 5.41 (s, 2 H). MS: (M[+]H m/z = 280.2).

N-Methoxy-N-methyl-4-(quinolin-2-ylmethoxy)-benzamide (6). To a solution of 4-(quinolin-2-ylmethoxy)-benzoic acid **5** (25.98 g, 93 mmol) was added 250 mL of thionyl chloride under N$_2$. The reaction mixture stirred 3 h, and the excess thionyl chloride was removed under vacuum. The acid chloride was dissolved in tetrahydrofuran (450 mL), and triethylamine (50 mL, 4 equiv) was slowly added. *O,N*-Dimethyl hydroxyl amine hydrochloride (27 g, 3 equiv) was added and the reaction stirred for 18 h. The reaction mixture was placed on a rotovap to remove the solvent, partitioned between 1 N NaOH and methylene chloride, separated, dried with magnesium sulfate, filtered, and concentrated. The crude product was filtered through silica gel eluting with 30−70% ethyl acetate/hexane to proved the title compound as a brown oil (26.26 g, 87%). ^{1}H NMR (400 MHz, CDCl$_3$) δ 8.17 (d, J = 8.7 Hz, 1 H), 8.06 (d, J = 8.3 Hz, 1 H), 7.81 (d, J = 8.3 Hz, 1H), 7.67 (m, 3 H), 7.63 (d, J = 8.3 Hz, 1 H), 7.52 (m, 1 H), 7.01 (M, 2 H), 5.39 (s, 2 H), 3.52 (s, 3 H) 3.31 (s, 2H). MS: (M[+]H m/z = 323.2).

2-Pyridin-4-yl-1-[4-(quinolin-2-ylmethoxy)-phenyl]-ethanone (7). To a solution of lithium diisopropyl amide (1.0M) in tetrahydrofuran was added 4-picoline dropwise (7.55 mL, 5 equiv) at 0 °C under N$_2$. After 30 min, the anion was cooled to −78 °C. In a separate round-bottom flask, *N*-methoxy-*N*-methyl-4-(quinolin-2-ylmethoxy)-benzamide **6** (5.0, 15.5 mmol) was dissolved in tetrahydrofuran (77 mL, 0.2M) and cooled to −78 °C under N$_2$. Then 1.2 equiv of the 4-picoline anion was added dropwise to the amide solution. After 45 min, 1 equiv more of the 4-picoline anion was added. After an additional 30 min, acetic acid (40 mL) was added dropwise and the reaction was slowly warmed to ambient temperature. The solid product (acetate salt) was filtered and partitioned between saturated sodium bicarbonate and dichloromethane. The layers were separated, dried with magnesium sulfate, filtered, and concentrated to provide the title compound as a tan solid (4.41 g, 80%). ^{1}H NMR (400 MHz, CDCl$_3$) δ 8.52 (d, J = 5.8 Hz, 2 H), 8.19 (d, J = 8.7 Hz, 1 H), 8.07 (d, J = 8.7 Hz, 1H), 7.93 (m, 2 H), 7.82 (d, J = 8.3 Hz, 1 H), 7.75 (m, 1 H), 7.61 (d, J = 8.3 Hz, 1 H), 7.54 (dt, J = 7.9, 1.0 Hz, 1 H), 7.23 (m, 2 H) 7.07 (m, 2H), 5.42 (s, 2H), 4.19 (s, 2H). MS: (M[+]H m/z = 355.2).

3-Dimethylamino-2-pyridin-4-yl-1-[4-(quinolin-2-ylmethoxy)-phenyl]-propenone (8). To 2-pyridin-4-yl-1-[4-(quinolin-2-ylmethoxy)-phenyl]-ethanone **7** (4.0 g, 11.3 mmol) was added dimethoxymethyl-dimethyl amine (10 mL) and the reaction mixture was heated at reflux for 1 h. The reaction mixture was concentrated to give a quantitative yield of the title compound, which was used without purification in the next step. LC/MS: RT = 1.4 min. MS: (M[+]H m/z = 410.2).

2-[4-(4-Pyridin-4-yl-2H-pyrazol-3-yl)-phenoxymethyl]-quinoline (3). To a solution of 3-dimethylamino-2-pyridin-4-yl-1-[4-(quinolin-2-ylmethoxy)-phenyl]-propenone **8** (9.57 g, 27 mmol) in methanol was added hydrazine hydrate (3.33 g, 40.5 mmol) and the reaction mixture was heated at reflux for 1 h. The solvent was evaporated to yield a white solid. The solid was washed with water and ethyl ether. The solid was recrystallized from hot ethanol/ethylacetate (10 mL/g) to give 8.34 g of the title compound (82%). ^{1}H NMR (400 MHz, DMSO) δ 8.41 (m, 3 H), 8.16 (s, 1 H), 7.97 (m, 2H), 7.86 (s, 1 H), 7.75 (t, J = 7.9 Hz, 1 H), 7.68 (d, J = 8.3 Hz, 1 H), 7.60 (t, J = 7.5 Hz, 1 H), 7.33 (m, 2 H), 7.18 (m, 2 H) 7.15 (d, J = 8.3 Hz, 1H), 7.06 (d, J = 8.3 Hz, 1H), 5.38 (s, 2H). MS: (M[+]H m/z = 379.2). Anal. Calcd for C$_{24}$H$_{18}$N$_4$O: C, 76.17%; H, 4.79%; N, 14.81%. Found: C, 75.82%; H, 4.73%; N, 14.71%.

2-[4-(1-Methyl-4-pyridin-4-yl-1H-pyrazol-3-yl)-phenoxymethyl]-quinoline (9). To a solution of 3-dimethylamino-2-pyridin-4-yl-1-[4-(quinolin-2-ylmethoxy)-phenyl]-propenone **8** (1.72 g) in ethanol (20 mL) was added methyl hydrazine (3.5 mL, 1.5 equiv) and concentrated sulfuric acid (0.1 mL). The reaction mixture was stirred 1 h at ambient temperature and solvent evaporated. The reaction mixture was partitioned between methylene chloride and saturated sodium bicarbonate. The layers were separated and the organic layer dried with magnesium sulfate, filtered, and concentrated. Preparative HPLC chromatography provided the title compound (major isomer) as a clear oil (0.97 g, 56%). ^{1}H NMR (400 MHz, CDCl$_3$) δ 8.44 (d, J = 5.0 Hz, 2 H), 8.17 (d, J = 8.7 Hz, 1 H), 8.05 (d, J = 8.3 Hz, 1H), 7.81 (d, J = 7.9 Hz, 1 H), 7.70 (m, 1 H), 7.66 (d, J = 8.7 Hz, 1H), 7.54 (s, 1H), 7.53 (m, 1H), 7.37 (d, J = 8.7 Hz, 2H) 7.15 (d, J = 5.0, 2H), 7.00 (d, J = 8.7 Hz, 2H), 5.38 (s, 2H), 3.93 (s, 3H). MS: (M[+]H m/z = 393.3). The free base was dilute in ethyl acetate, and a suspension of succinic acid (1 equiv) in ethyl acetate was added. The mixture was stirred overnight, then filtered and washed with ether to provide the succinate salt. ^{1}H NMR (500 MHz, methanol-d_4) δ ppm 2.57 (s, 4 H) 3.96 (s, 3 H) 5.41 (s, 2 H) 7.11 (d, J = 8.79 Hz, 2 H) 7.30 (d, J = 6.35 Hz, 2 H) 7.36 (d, J = 8.79 Hz, 2 H) 7.59−7.65 (m, 1 H) 7.75 (d, J = 8.54 Hz, 1 H) 7.80 (ddd, J = 8.48, 6.89, 1.46 Hz, 1 H) 7.95 (d, J = 1.22 Hz, 1 H) 8.02 (s, 1 H) 8.06 (d, J = 8.54 Hz, 1 H) 8.36 (dd, J = 4.76, 1.59 Hz, 2 H) 8.40 (d, J = 8.54 Hz, 1 H) MS: (M[+]H m/z=510.6). Anal. Calcd for C$_{24}$H$_{18}$N$_4$O·C$_4$H$_6$O$_4$: C, 68.22%; H, 5.13%; N, 10.97%. Found: C, 68.05%; H, 4.99%; N, 10.87%.

2-[4-(2-Methyl-4-pyridin-4-yl-2H-pyrazol-3-yl)-phenoxymethyl]-quinoline (10). To a solution of 3-dimethylamino-2-pyridin-4-yl-1-[4-(quinolin-2-ylmethoxy)-phenyl]-propenone **8** (1.72 g) in ethanol (20 mL) was added methyl hydrazine (3.5 mL, 1.5 equiv) and concentrated sulfuric acid (0.1 mL). The reaction mixture was stirred 1 h at ambient temperature followed by solvent evaporation. The reaction mixture was partitioned between methylene chloride and saturated sodium bicarbonate. The layers were separated and the organic layer dried with magnesium sulfate, filtered, and concentrated. Preparative HPLC chromatography provided the title compound (minor isomer) as a white solid (0.30 g, 17%). ^{1}H NMR (400 MHz, CDCl$_3$) δ 8.31 (d, J = 5.4 Hz, 2 H), 8.21 (d, J = 8.7 Hz, 1 H), 7.80 (d, J = 8.3 Hz, 1H), 7.77 (s, 1 H), 7.66 (m, 3 H), 7.53 (m, 1H), 7.19 (d, J = 8.7 Hz, 2 H), 7.11 (d, J = 8.7 Hz, 2 H), 7.01 (d, J = 6.2 Hz, 2H) 5.40 (s, 2H), 3.69 (s, 3H). MS: (M[+]H m/z = 393.3). HPLC purity, column 4: RT 2.764, 96.76%.

2-[4-(1-Ethyl-4-pyridin-4-yl-1H-pyrazol-3-yl)-phenoxymethyl]-quinoline (11). Following the procedure for the preparation of 2-[4-(1-methyl-4-pyridin-4-yl-1H-pyrazol-3-yl)-phenoxymethyl]-quinoline **9** but substituting ethyl hydrazine provided the title compound (37%). ^{1}H NMR (400 MHz, CDCl$_3$) δ 8.35 (bs, 2H), 8.19 (d, J = 8.3 Hz, 1 H), 8.07 (d, J = 9.1 Hz, 1 H), 7.82 (d, J = 7.9 Hz, 1H), 7.73 (t, J = 8.3 Hz, 1H), 7.67 (d, J = 8.3 Hz, 2 H), 7.62 (s, 1H), 7.55 (t, J = 7.9 Hz, 1 H), 7.37 (d, J = 9.1 Hz, 2H), 7.21 (bs, 2 H), 7.01 (d, J = 8.7 Hz, 2H) 5.39 (s, 2H), 4.24 (q, J = 7.5 Hz, 2H), 1.56 (t, J = 7.5 Hz, 3H). MS: (M[+]H m/z = 407.3). HPLC purity, column 4: RT 3.007, 95.73%.

2-[4-(2-Ethyl-4-pyridin-4-yl-2H-pyrazol-3-yl)-phenoxymethyl]-quinoline (12). Following the procedure for the preparation of 2-[4-(1-methyl-4-pyridin-4-yl-1H-pyrazol-3-yl)-phenoxymethyl]-quinoline **9** but substituting ethyl hydrazine provided the title compound (33%). ^{1}H NMR (400 MHz, CDCl$_3$) δ 8.35 (bs, 2H), 8.23 (d, J = 8.3 Hz, 1 H), 8.08 (d, J = 8.3 Hz, 1 H), 7.85 (d, J = 7.4 Hz, 1H), 7.83 (s, 1 H), 7.74 (m, 2 H), 7.57 (t, J = 7.9 Hz, 1H), 7.21 (d, J = 8.7 Hz, 2 H), 7.14 (d, J = 9.1 Hz, 2 H), 7.04 (m, 2H) 5.42 (s, 2H), 4.03 (q, J = 7.5 Hz, 2H), 1.36 (t, J = 7.5 Hz, 3H). MS: (M[+]H m/z = 407.3). HPLC purity, column 4: RT 2.977, 99.00%.

2-{4-[-Pyridin-4-yl-1-(2,2,2-trifluoro-ethyl)-1H-pyrazol-3-yl]-phenoxymethyl}-quinoline (13). Following the procedure for the preparation of 2-[4-(1-methyl-4-pyridin-4-yl-1H-pyrazol-3-yl)-phenoxymethyl]-quinoline **9** but substituting (2,2,2-trifluoro-ethyl)-hydrazine provided the title compound (58%). MS: (M[+]H m/z = 461.2). The free base was diluted in ethyl acetate, and a suspension of succinic acid (1 equiv) in ethyl acetate was added. The mixture was stirred overnight, then filtered to provide the hemisalt. ^{1}H NMR (500 MHz, methanol-d_4) δ ppm 2.57 (s, 2 H) 5.01 (q, J = 8.54 Hz, 3 F) 5.40 (s, 2 H)

7.11 (d, $J = 9.03$ Hz, 2 H) 7.31 (d, $J = 6.10$ Hz, 2 H) 7.38 (d, $J = 9.03$ Hz, 2 H) 7.60−7.64 (m, 1 H) 7.75 (d, $J = 8.54$ Hz, 1 H) 7.79 (ddd, $J = 8.42, 6.96, 1.46$ Hz, 1 H) 7.96 (dd, $J = 8.30, 1.22$ Hz, 1 H) 8.05 (d, $J = 8.54$ Hz, 1 H) 8.17 (s, 1 H) 8.40 (d, $J = 1.46$ Hz, 2 H) 8.39 (t, $J = 2.44$ Hz, 2 H). MS: (M^+H m/z = 519.51). Anal. Calcd for $C_{26}H_{19}N_4OF_3 \cdot C_4H_6O_4$: C, 64.74%; H, 4.27%; N, 10.78%; F, 10.97%. Found: C, 64.63%; H, 4.12%; N, 10.72%; F, 11.00%.

2-[4-(4-Pyridin-4-yl-isoxazol-5-yl)-phenoxymethyl]-quinoline (14). 2-Pyridin-4-yl-1-[4-(quinolin-2-ylmethoxy)-phenyl]-ethanone **7** (200 mg, 0.56 mmol) was heated at reflux in dimethoxymethyl-dimethyl amine (1 mL) for 1 h and concentrated. The crude product was dissolved in methanol/water (3:1, 4 mL), and hydroxyl amine hydrochloride (43 mg, 1.1 equiv) was added. After 1 h, acetic acid was added (0.016 mL) and the reaction was heated at reflux for 1 h, cooled to ambient temperature, poured into saturated sodium bicarbonate, extracted with methylene chloride, dried with magnesium sulfate, filtered, and concentrated. Biotage MPLC was run on a 25S column elution with 3% methanol/1%ammonium hydroxide/ethyl acetate 50% in hexanes to provide the title compound as a tan solid (94 mg, 45%). ^{1}H NMR (400 MHz, CDCl$_3$) δ 8.59 (dd, $J = 6.2, 1.7$ Hz, 2 H), 8.36 (s, 1H), 8.20 (d, $J = 8.3$ Hz, 1H), 8.07 (d, $J = 8.7$ Hz, 1 H), 7.82 (d, $J = 9.1$ Hz, 1 H), 7.73 (dt, $J = 7.1, 1.7$ Hz, 1H), 7.64 (d, $J = 8.3$ Hz, 1H), 7.54 (m, 3H), 7.28 (d, $J = 4.2$ Hz, 2H) 7.05 (d, $J = 9.1$, 2H), 5.40 (s, 2H). MS: (M^+H m/z = 380.2). HPLC purity, column 5: RT 4.467, 99.08%.

2-[4-(2-Methyl-5-pyridin-4-yl-pyrimidin-4-yl)-phenoxymethyl]-quinoline (15). Following the procedure for the preparation of 2-[4-(5-pyridin-4-yl-pyrimidin-4-yl)-phenoxymethyl]-quinoline but substituting acetamidine hydrochloride provide the title compound (58%). ^{1}H NMR (400 MHz, CDCl$_3$) δ 9.21 (s, 1H), 8.63 (S, 1H), 8.58 (m, 2 H), 8.17 (d, $J = 8.7$ Hz, 1H), 8.04 (d, $J = 8.7$ Hz, 1H), 7.81 (d, $J = 8.3$ Hz, 1 H), 7.70 (m, 1 H), 7.60 (d, $J = 8.3$ Hz, 1H), 7.52 (m, 1H), 7.37 (m, 2H) 7.15 (d, $J = 6.2$, 2H), 6.93 (d, $J = 9.1$ Hz, 2H), 5.35 (s, 2H). MS: (M^+H m/z = 405.2). HPLC purity, column 1: RT 3.050, 97.98%.

2-[-4-(4-Pyrimidin-4-yl-2H-pyrazol-3-yl)-phenoxymethyl]-quinoline (16). Following the procedure for the preparation of 2-[4-(4-pyridin-4-yl-2H-pyrazol-3-yl)-phenoxymethyl]-quinoline **3** and substituting 4-methylpyrimidine for 4-picoline provided the title compound as a white solid (75%). ^{1}H NMR (400 MHz, methanol-d_4) d ppm 5.41 (s, 2 H) 7.16 (br s, 4 H) 7.43 (br s, 2 H) 7.59 (s, 1 H) 7.68−7.83 (m, 2 H) 7.92 (s, 1 H) 8.02 (s, 1 H) 8.36 (s, 1 H) 8.44 (s, 1 H) 8.96 (d, $J = 1.17$ Hz, 1 H). LC/MS: RT = 1.8 min. MS: (M^+H m/z = 380.2). HPLC purity, column 4: RT 2.790, 99.52%.

2-[4-(4-Pyridazin-4-yl-2H-pyrazol-3-yl)-phenoxymethyl]-quinoline (17). Following the procedure for the preparation of 2-[-4-(4-pyridin-4-yl-2H-pyrazol-3-yl)-phenoxymethyl]-quinoline **3** but substituting 4-methyl pyridazine for 4-picoline provided the title compound as a white solid (32%). ^{1}H NMR (400 MHz, CDCl$_3$) δ 9.11 (s, 1H), 9.01 (d, $J = 5.0$ Hz, 1H), 8.34 (d, $J = 8.7$ Hz, 1 H), 8.25 (d, $J = 8.7$ Hz, 1H), 7.89 (m 2H), 7.81 (d, $J = 8.3$ Hz, 1 H), 7.79 (m, 2 H), 7.61 (t, $J = 7.6$ Hz, 1H), 7.34 (m, 1H), 7.31 (d, $J = 8.7$ Hz, 2H), 7.05 (d, $J = 8.7$, 2H), 5.49 (s, 2H). MS: (M^+H m/z = 380.2). HPLC purity, column 5: RT 3.433, 95.51%.

2-((4-(4-phenyl-1H-pyrazol-5-yl)phenoxy)methyl)quinoline (18). Following the procedure for the preparation of 2-[4-(4-pyridin-4-yl-2H-pyrazol-3-yl)-phenoxymethyl]-quinoline **3** and substituting toluene for 4-picoline provided the title compound (38%). ^{1}H NMR (400 MHz, methanol-d_4) δ ppm 5.34 (s, 2 H) 7.02 (d, $J = 8.78$ Hz, 2H) 7.22 (d, $J = 4.49$ Hz, 4 H) 7.12−7.25 (m, 2H) 7.32 (d, $J = 8.98$ Hz, 2 H) 7.58 (ddd, $J = 8.15, 6.98, 1.07$ Hz, 1 H) 7.69 (d, $J = 8.39$ Hz, 2 H) 7.75 (ddd, $J = 8.44, 6.98, 1.56$ Hz, 1 H) 7.91 (dd, $J = 8.20, 1.37$ Hz, 1 H) 8.01 (dd, $J = 8.59, 0.98$ Hz, 1 H) 8.34 (d, $J = 8.39$ Hz, 1 H). MS (LC/MS) = 378.1 (M + H). HPLC purity, column 4: RT 4.156, 97.77%.

2-((4-(4-(pyridin-2-yl)-1H-pyrazol-5-yl)phenoxy)methyl)quinoline (19). Following the procedure for the preparation of 2-[-4-

(4-pyridin-4-yl-2H-pyrazol-3-yl)-phenoxymethyl]-quinoline **3** and substituting 2-methyl pyridine for 4-picoline provided the title compound (53%). ^{1}H NMR (400 MHz, methanol-d_4) d ppm 5.37 (br s, 2 H) 7.08 (br s, 2 H) 7.20 (ddd, $J = 7.46, 5.03, 0.98$ Hz, 2 H) 7.35 (d, $J = 8.78$ Hz, 2 H) 7.55−7.65 (m, 2 H) 7.68−7.81 (m, 2 H) 7.71 (d, $J = 8.39$ Hz, 1H) 7.92 (dd, $J = 8.20, 1.17$ Hz, 1 H) 8.01 (d, $J = 8.59$ Hz, 1 H) 8.36 (d, $J = 8.39$ Hz, 1 H) 8.45 (ddd, $J = 4.98, 1.85, 0.98$ Hz, 1 H). MS (LC/MS) = 379.1 (M + H). HPLC purity, column 2: RT 4.040, 99.28%.

2-{4-[4-(3-Methyl-isoxazol-5-yl)-2H-pyrazol-3-yl]-phenoxymethyl}-quinoline (20). Following the procedure for the preparation of 2-[4-(4-pyridin-4-yl-2H-pyrazol-3-yl)-phenoxymethyl]-quinoline **3** and substituting 3,5-dimethyl isoxazole for 4-picoline provided the title compound (43%). ^{1}H NMR (400 MHz, CDCl$_3$) δ 8.23 (d, $J = 8.7$ Hz, 1H), 8.12 (d, $J = 8.7$ Hz, 1H), 7.94 (s, 1 H), 7.84 (d, $J = 7.1$ Hz, 1H), 7.74 (m, 1H), 7.69 (d, $J = 8.3$ Hz, 1 H), 7.57 (t, $J = 6.6$ Hz, 2 H), 7.46 (d, $J = 8.7$ Hz, 2H), 7.08 (d, $J = 8.7$ Hz, 2H), 5.88 (s, 1H), 5.42 (s, 2H), 2.23 (s, 3H). MS: (M^+H m/z = 383.2). HPLC purity, column 1: RT 3.660, 96.23%.

4-Benzyloxy-N-methoxy-N-methyl-benzamide. Following the procedure for the preparation of N-methoxy-N-methyl-4-(quinolin-2-ylmethoxy)-benzamide **6** but substituting 4-benzyloxy benzoic acid **21** provided the title compound as a waxy solid (99%). ^{1}H NMR (400 MHz, CDCl$_3$) δ 7.75 (s, 2H), 7.65 (d, $J = 9.1$ Hz, 1H), 7.33 (m, 5H), 6.93 (d, $J = 9.1$ Hz, 1H), 5.05 (s, 2H), 3.52 (s, 3H), 3.30 (s, 3H). MS: (M^+H m/z = 272.3).

1-(4-Benzyloxy-phenyl)-2-pyridin-4-yl-ethanone (22). Following the procedure for the preparation of 2-pyridin-4-yl-1-[4-(quinolin-2-ylmethoxy)-phenyl]-ethanone **7** but substituting 4-benzyloxy-N-methoxy-N-methyl-benzamide provided the title compound (73%). ^{1}H NMR (400 MHz, CDCl$_3$) δ 8.53 (d, $J = 5.8$ Hz, 2H), 7.95 (d, $J = 9.1$ Hz, 2H), 7.36 (m, 5H), 7.17 (d, $J = 6.2$ Hz, 2H) 7.01 (d, 9.1 Hz, 2H), 5.12 (s, 2H), 4.21 (s, 2H). MS: (M^+H m/z = 304.2).

4-[3-(4-Benzyloxy-phenyl)-1-methyl-1H-pyrazol-4-yl]-pyridine (23). Following the procedure for the preparation of 2-[4-(1-methyl-4-pyridin-4-yl-1H-pyrazol-3-yl)-phenoxymethyl]-quinoline **9** but substituting 1-(4-benzyloxy-phenyl)-2-pyridin-4-yl-ethanone **22** provided the title compound (45%). ^{1}H NMR (400 MHz, CDCl$_3$) δ 8.45 (d, $J = 6.2$ Hz, 2H), 7.36 (m, 8H), 7.15 (d, $J = 6.2$ Hz, 2H), 6.94 (d, $J = 8.7$ Hz, 2H), 5.06 (s, 2H), 3.96 (s, 3H). MS: (M^+H m/z = 342.2).

4-(1-Methyl-4-pyridin-4-yl-1H-pyrazol-3-yl)-phenol (24). To a solution of 4-[3-(4-benzyloxy-phenyl)-1-methyl-1H-pyrazol-4-yl]-pyridine **23** (1.28 g) in ethanol (50 mL)/ethyl acetate (50 mL) in a parr bottle was added palladium hydroxide (500 mg). The parr bottle was charged to 40 psi on a shaker for 6 h. The reaction mixture was filtered and concentrated. MPLC biotage chromatography eluting with methanol (1−7%)/chloroform provided the title compound (860 mg, 91%). ^{1}H NMR (400 MHz, DMSO) δ 9.53 (s, 1H), 8.39 (d, $J = 5.8$ Hz, 2 H), 7.15 (m, 4H), 6.72 (d, $J = 8.7$ Hz, 1H), 3.84 (s, 3H). MS: (M^+H m/z = 252.2).

2-[4-(1-Methyl-4-pyridin-4-yl-1H-pyrazol-3-yl)-phenoxymethyl]-quinoxaline (25). To a solution of 4-(1-methyl-4-pyridin-4-yl-1H-pyrazol-3-yl)-phenol **24** (50 mg) in dioxane (2 mL) was added triphenylphosphine (84 mg), quinoxaline-2-yl-methanol (48 mg), and di-t-butyl-aza-dicarboxylate (73 mg) and the reaction mixture was heated at 60 °C for 18 h. The reaction mixture was poured into 1 N NaOH, extracted 3× methylene chloride, dried with magnesium sulfate, filtered, and concentrated. Purification via MPLC biotage chromatography provided the title compound (54 mg, 67%). ^{1}H NMR (400 MHz, CDCl$_3$) δ 9.09 (s, 1H), 8.45 (d, $J = 6.2$ Hz, 2H), 8.10 (m, 2 H), 7.77 (m, 2H), 7.55 (s, 1H), 7.37 (d, $J = 9.1$ Hz, 2H), 7.10 (d, $J = 6.9$ Hz, 2 H), 7.01 (d, $J = 8.7$ Hz, 2H), 5.41 (s, 2 H), 3.94 (s, 3H). MS: (M^+H m/z = 394.4)). HPLC purity, column 5: RT 3.660, 98.64%.

1-Methyl-2-[4-(1-methyl-4-pyridin-4-yl-1H-pyrazol-3-yl)-phenoxymethyl]-1H-benzoimidazole (26). To a solution of 4-(1-methyl-4-pyridin-4-yl-1H-pyrazol-3-yl)-phenol (50 mg) in dioxane (1 mL)

was added triphenyl phosphine (83 mg), (1-methyl-1*H*-benzoimidazol-2-yl)-methanol (48 mg) and di-*t*-butyl azodicarboxylate (73 mg). The reaction mixture was heated at 60 °C for 18, poured into 1 N NaOH, extracted 3× with chloroform, dried with magnesium sulfate, filtered, and concentrated. Purification via biotage MPLC eluting with 80% ethyl acetate/hexane provided the title compound (75 mg, 96%). ^{1}H NMR (400 MHz, CDCl$_3$) δ 8.44 (d, $J = 6.2$ Hz, 2 H), 7.76 (dd, $J = 7.1$, 1.7 Hz, 1 H), 7.55 (s, 1H), 7.37−7.28 (m, 5 H), 7.15 (dd, $J = 4.6$, 1.7 Hz, 2H), 7.05 (d, $J = 9.1$ Hz, 2H), 5.38 (s, 2H), 3.94 (s, 3H) 3.88 (s, 3H). MS: (M$^+$H $m/z = 396.2$). The free base was dilute in ethyl acetate and a suspension of succinic acid (1 equiv) in ethyl acetate was added. The mixture was stirred overnight, and the filtrates were washed with ether to provide the succinic acid salt. Anal. Calcd for C$_{24}$H$_{21}$N$_5$O·C$_4$H$_6$O$_4$: C, 65.49%; H, 5.30%; N, 13.64%. Found: C, 65.49%; H, 5.30%; N, 13.45%.

2-[4-(1-Methyl-4-pyridin-4-yl-1*H*-pyrazol-3-yl)-phenoxymethyl]-imidazo[1,2-*a*]pyridine (27). Following the procedure for the preparation of 1-methyl-2-[4-(1-methyl-4-pyridin-4-yl-1*H*-pyrazol-3-yl)-phenoxymethyl]-1*H*-benzoimidazole **26** but substituting imidazo[1,2-*a*]pyridin-2-yl-methanol provided the title compound (74%). ^{1}H NMR (400 MHz, CDCl$_3$) δ 8.48 (d, $J = 6.2$, 2 H), 7.87 (d, $J = 7.1$ Hz, 1H), 7.60 (d, $J = 9.1$ Hz, 1H), 7.57 (s, 1H), 7.38 (t, $J = 8.7$ Hz, 2 H), 7.18 (d, $J = 6.2$ Hz, 2H), 7.04 (d, $J = 8.7$ Hz, 2H), 6.86 (d, $J = 6.6$ Hz, 1H), 5.28 (s, 2H), 3.97 (s, 3H) 2.52 (s, 3H). MS: (M$^+$H $m/z = 382.1$). HPLC purity, column 1: RT 3.660, 99.20%.

2-[4-(1-Methyl-4-pyridin-4-yl-1*H*-pyrazol-3-yl)-phenoxymethyl]-[1,2,4]triazolo[1,5-*a*]-pyridine (28). Following the procedure for the preparation of 1-methyl-2-[4-(1-methyl-4-pyridin-4-yl-1*H*-pyrazol-3-yl)-phenoxymethyl]-1*H*-benzoimidazole **26** but substituting [1,2,4]triazolo[1,5-*a*]pyridin-2-yl-methanol provided the title compound (91%). 8.57 (d, $J = 6.6$ Hz, 1 H), 8.44 (d, $J = 5.8$ Hz, 2H), 7.73 (d, $J = 9.1$ Hz, 1H), 7.55 (s, 1H), 7.54 (dd, $J = 6.6$, 1.3 Hz, 1 H), 7.38 (d, $J = 8.7$ Hz, 2H), 7.14 (d, $J = 5.8$ Hz, 2H), 7.05 (m, 3H), 5.36 (s, 2H), 3.94 (s, 3H). MS: (M$^+$H $m/z = 383.1$). HPLC purity, column 2: RT 3.143, 99.01%.

Supporting Information Available: Crystal structure data, in vitro biology data with statistics, biological experimentals, and pharmacokinetic experimentals are provided. This material is available free of charge via the Internet at http://pubs.acs.org.

References

(1) Setter, S. M.; Iltz, J. L.; Fincham, J. E.; Campbell, R. K.; Baker, D. E. Phosphodiesterase 5 Inhibitors for Erectile Dysfunction. *Ann. Pharmacol.* **2005**, *39* (7/8), 1286–1295.

(2) Manallack, D. T.; Hughes, R. A.; Thompson, P. E. The Next Generation of Phosphodiesterase Inhibitors: Structural Clues to Ligand and Substrate Selectivity of Phosphodiesterases. *J. Med. Chem.* **2005**, *48* (10), 3449–3462.

(3) Seeger, T. F.; Bartlett, B.; Coskran, T. M.; Culp, J. S.; James, L. C.; Krull, D. L.; Lanfear, J.; Ryan, A. M.; Schmidt, C. J.; Strick, C. A.; Varghese, A. H.; Williams, R. D.; Wylie, P. G.; Menniti, F. S. Immunohistochemical Localization of PDE10A in the Rat Brain. *Brain Res.* **2003**, *985*, 113–126.

(4) Fujishige, K.; Kotera, J.; Michibata, H.; Yuasa, K.; Takebayashi, S.; Okumura, K.; Omori, K. Cloning and Characterization of a Novel Human Phosphodiesterase that Hydrolyzes Both cAMP and cGMP (PDE10A). *J. Biol. Chem.* **1999**, *274* (26), 18438–18445.

(5) Schmidt, C. J.; Chapin, D. S.; Cianfrogna, J.; Corman, M. L.; Hajos, M.; Harms, J. F.; Hoffman, W. E.; Lebel, L. A.; McCarthy, S. A.; Nelson, F. R.; Proulx-LaFrance, C.; Majchrzak, A. D.; Ramirez, A. D.; Schmidt, K.; Seymour, P. A.; Siuciak, J. A.; Tingley, F. D., III; Williams, R. D.; Verhoest, P. R.; Menniti, F. S. Preclinical Characterization of Selective Phosphodiesterase 10A Inhibitors: A New Therapeutic Approach to the Treatment of Schizophrenia. *J. Pharm. Exp. Ther.* **2008**, *325* (2), 681–690.

(6) Card, G. L.; England, B. P.; Suzuki, Y.; Fong, D.; Powell, B.; Lee, B.; Luu, C.; Tabrizizad, M.; Gillete, S.; Ibrahim, P. N.; Artis, D. R.; Bollag, G.; Milburn, M. V.; Kim, S.; Schlessinger, J.; Zang, K. Y. J. Structural Basis for the Activity of Drugs that Inhibit Phosphodiesterases. *Structure* **2004**, *12*, 2233–2247.

(7) Cote, R. H.; Feng, Q.; Valeriani, B. A. Relative Potency of Various Classes of Phosphodiesterase (PDE) Inhibitors for Rod and Cone Photoreceptor PDE6. *Invest. Ophthalmol.* **2003**, *44*, 1524–1527.

(8) Young, R. A.; Ward, A. Milrinone. A Preliminary Review of its Pharmacological Properties and Therapeutic Use. *Drugs* **1988**, *36* (2), 158–192.

(9) Chappie, T. A.; Humphrey, J. M.; Allen, M. P.; Estep, K. G.; Fox, C. B.; Lebel, L. A.; Liras, S.; Marr, E. S.; Menniti, F. S.; Pandit, J.; Schmidt, C. J.; Tu, M.; Williams, R. D.; Yang, F. V. Discovery of a Series of 6,7-Dimethoxy-4-pyrrolidylquinazoline PDE10A Inhibitors. *J. Med. Chem.* **2007**, *50* (2), 182–185.

(10) Seko, N.; Yoshino, K.; Yokota, K.; Tsukamoto, G. Synthesis and Platelet Aggregation Inhibitory Activity of Diphenylazole Derivatives. I. Thiazole and Imidazole Derivatives. *Chem. Pharm. Bull.* **1991**, *39* (3), 651–657.

(11) Biot, C.; Buisine, E.; Rooman, M. Free-Energy Calculations of Protein−Ligand Cation and Amino Interactions: From Vacuum to Protein Like Environments. *J. Am. Chem. Soc.* **2003**, *125* (46), 13988–13994.

(12) Lipinski, C. A.; Lombardo, F.; Dominy, B. W.; Feeney, P. J. Experimental and Computational Approaches to Estimate Solubility in Drug Discovery and Development Settings. *Adv. Drug Delivery Rev.* **1997**, *23*, 3–25.

(13) Melnikov, P.; Corbi, P. P.; Cuin, A.; Cavicchioli, M.; Guimaraes, W. R. Physicochemical Properties of Sidenafil Citrate and Sidenafil Base. *J. Pharm. Sci.* **2003**, *92* (10), 2140–2143.

(14) Hopkins, A. L.; Groom, C. R.; Alex, A. Ligand Efficiency: A Useful Metric for Lead Selection. *Drug Discovery Today* **2004**, *9* (10), 430–431.

(15) Nahm, S.; Wienreb, S. M. *N*-Methoxy-*N*-Methylamides as Effective Acylating Agents. *Tetrahedron Lett.* **1981**, *22* (39), 3815–3818.

(16) Zlokarnik, G.; Grootenhuis, P. D. J.; Watson, J. B. High Throughput P450 Inhibition Screens in Early Drug Discovery. *Drug Discovery Today* **2005**, *10* (21), 1443–1450.

(17) Siuciak, J. A.; Chapin, D. S.; Harms, J. F.; Lebel, L. A.; McCarthy, S. A.; Chambers, L.; Shirkhande, A.; Wong, S.; Menniti, F. S.; Schmidt, C. J. Inhibition of Striatal-Enriched Phosphodiesterase 10A: A Novel Approach for the Treatment of Psychosis. *Neuropharmacology* **2006**, *51* (2), 374–385.

(18) Verhoest, P. R.; Helal, C. J.; Hoover, D. J.; Humphrey, J. M. Heteroaromatic Quinoline Compounds as Phosphodiesterase Inhibitors, their Preparation, Pharmaceutical Compositions, and Use in Therapy. Patent WO 2006072828, July 13, **2006**.

(19) Feng, B; Mills, J.; Davidson, R. E.; Mireles, R. J.; Janiszewski, J. S.; Troutman, M. D.; de Morais, S. M. In Vitro P-glycoprotein Assays to Predict the In Vivo Interactions of P-glycoprotein with Drugs in the Central Nervous System. *Drug Metab. Dispos.* **2008**, *36* (2), 268–275.

(20) Kaminski, G. A.; Maple, J. R.; Murphy, R. B.; Braden, D. A.; Friesner, R. A. *J. Chem. Theory Comput.* **2005**, *1* (2), pp 248−254.

(21) Jaguar, Schrodinger, Inc.

(22) Kuntz, I. D.; Chen, K.; Sharp, K. A.; Kollman, P. A. The Maximal Affinity of Ligands. *Proc. Natl. Acad. Sci. U.S.A.* **1999**, *96* (18), 9997–10002.

(23) See www.pfizer.com/research/. Accessed on 07/23/2009.